AD-A071 087 NAVAL RESEARCH LAB WASHINGTON DC F/G 20/5
THE ELECTRON CYCLOTRON MASER AS A HIGH-POWER TRAVELLING-WAVE AM--ETC(U)
JUN 79 J L SEFTOR, V L GRANATSTEIN, K R CHU
UNCLASSIFIED NRL-MR-3989 NL

| OF |

AD
A071087

END
DATE
FILMED
8 --79
DDC

NRL Memorandum Report 3989

The Electron Cyclotron Maser as a High-Power Travelling-Wave Amplifier of Millimeter Waves

J. L. SEFTOR, V. L. GRANATSTEIN, K. R. CHU, P. SPRANGLE, AND M. READ

Electron Beam Applications Branch
Plasma Physics Division

June 19, 1979

NAVAL RESEARCH LABORATORY
Washington, D.C.

SECURITY CLASSIFICATION OF THIS PAGE (When Data Entered)

REPORT DOCUMENTATION PAGE

READ INSTRUCTIONS BEFORE COMPLETING FORM

1. REPORT NUMBER: NRL Memorandum Report 3989

2. GOVT ACCESSION NO.

3. RECIPIENT'S CATALOG NUMBER: (9) (14) NRL-MR-3989

4. TITLE (and Subtitle): (6) THE ELECTRON CYCLOTRON MASER AS A HIGH-POWER TRAVELLING-WAVE AMPLIFIER OF MILLIMETER WAVES.

5. TYPE OF REPORT & PERIOD COVERED: Interim report on a continuing NRL problem.

6. PERFORMING ORG. REPORT NUMBER

7. AUTHOR(s): (10) J. L. Seftor*, V. L. Granatstein, K. R. Chu, P. Sprangle, and M. Read

8. CONTRACT OR GRANT NUMBER(s)

9. PERFORMING ORGANIZATION NAME AND ADDRESS: Naval Research Laboratory, Washington, DC 20375

10. PROGRAM ELEMENT, PROJECT, TASK AREA & WORK UNIT NUMBERS: NRL Problem R08-92 - XF54581007; NRL Problem R08-95 - W31RPD-93-Z082

11. CONTROLLING OFFICE NAME AND ADDRESS: Naval Electronic Systems Command, Washington, DC 20360 and Ballistic Missile Defense Advanced Technology Center, Huntsville, Alabama, 35807

12. REPORT DATE: June 19, 1979

13. NUMBER OF PAGES: 28

14. MONITORING AGENCY NAME & ADDRESS (if different from Controlling Office): (11) 19 Jun 79 (12) 29p.

15. SECURITY CLASS. (of this report): UNCLASSIFIED

15a. DECLASSIFICATION/DOWNGRADING SCHEDULE

16. DISTRIBUTION STATEMENT (of this Report)

Approved for public release; distribution unlimited.

17. DISTRIBUTION STATEMENT (of the abstract entered in Block 20, if different from Report)

18. SUPPLEMENTARY NOTES

*Present Address: Science Applications, Inc., McLean, Virginia 22101

Work supported by the Naval Electronic Systems Command, Task No. XF 54 581 007, and by the Army Ballistic Missile Advanced Technology Center, MIPR No. W3IRPD-93-Z082.

19. KEY WORDS (Continue on reverse side if necessary and identify by block number)

Electron cyclotron maser
Gyrotron travelling wave amplifier
Millimeter wavelengths

20. ABSTRACT (Continue on reverse side if necessary and identify by block number)

The electron cyclotron maser instability has been exploited as the basis for a new type of travelling wave amplifier which operates at unusually high power levels at millimeter wavelengths. The first experimental model of this amplifier has been operated at 35 GHz and has demonstrated a stable gain of 17 dB and an output power of 10 kW (unsaturated). The gain was linear over a dynamic range > 30 dB. The absolute value of the gain and its dependence on current and magnetic field were in excellent agreement with theoretical calculations. Bandwidth and saturated power

(Continues)

DD FORM 1 JAN 73 1473 EDITION OF 1 NOV 65 IS OBSOLETE
S/N 0102-014-6601

251 950

SECURITY CLASSIFICATION OF THIS PAGE (When Data Entered)

20. Abstract (Continued)

have yet to be measured directly but no fundamental problems were observed which will prevent successful achievement of the design predictions (viz., bandwidth $\simeq$ 10%, power on the order of 10^5 watts, efficiency > 10%).

APPROXIMATELY

100,000

CONTENTS

THE ELECTRON CYCLOTRON MASER AS A HIGH-POWER TRAVELLING-WAVE AMPLIFIER OF MILLIMETER WAVES

INTRODUCTION

Research studies of the electron cyclotron maser, both theoretical [1-5] and experimental [6-8] began two decades ago. These studies have now led to the development of an important new class of millimeter-wave oscillators known as gyrotrons [9]. The most outstanding results with gyrotron oscillator cavities have been reported by research workers in the Soviet Union; their results include the following: 1.5 kW, cw, at $\lambda = 0.9$ mm with 6% efficiency [10]; 22 kW, cw, at $\lambda = 2$ mm with 22% efficiency [11]; a 1.1 MW pulse at $\lambda = 3$ mm with 34% efficiency [11]; and a 1.25 MW pulse at 6.7 mm with 35% efficiency [11]. The pulse duration in the last two megawatt level experiments is believed to be 0.1 ms and 5 ms respectively [12]. Development of high-power gyrotron oscillators of the cw and long pulse variety is also underway in the United States [13, 14].

It is clear from the above that gyrotron oscillators have produced power levels that are orders of magnitude larger than previously available at millimeter wavelengths, and with good efficiency. These oscillators have already been applied to heating plasmas in controlled thermonuclear fusion research [15]. Although the gyrotron oscillator is well suited to heating applications, more sophisticated systems (e.g., communications, radar) require amplifiers with substantial instantaneous bandwidth.

Note: Manuscript submitted March 1, 1979.

In 1975, an experiment on the electron cyclotron maser instability in an intense relativistic electron beam demonstrated wideband amplification [16]. This led to a comprehensive nonlinear theory of the electron cyclotron maser as a travelling wave amplifier [17], and to the optimized design of such a device at a frequency of 35 GHz [18]. The design predicted that the type of high power and efficiency which characterizes gyrotron oscillators would also be obtainable in the gyrotron amplifier (viz., 340 kW at 51% efficiency), while at the same time, predicting a bandwidth of several percent. In this paper, we report the first operation of the gyrotron travelling wave amplifier which was constructed according to that optimized design.

PRINCIPLES OF OPERATION

Before proceeding with a specific discussion of the amplifier, we will outline for the readers' convenience the general principles underlying the operation of electron cyclotron masers. For simplicity, we will assume that the electrons are moving transverse to a steady magnetic field, $\underset{\sim}{B}_o$, and that the unquantized electron velocity component parallel to B_o is negligible.

The quantum mechanical description of the amplification of a fast electromagnetic wave by interaction with free electrons gyrating in a steady magnetic field comes from the work of Twiss [1] and Schneider [2]. Two necessary conditions for wave amplification have to be simultaneously satisfied [1]; viz.,

$$\partial f/\partial W > 0 \qquad (1)$$

and

$$\partial Q/\partial W < 0 \qquad (2)$$

where W is electron kinetic energy, f(W) is the electron distribution function, and Q(W) is the transition probability for stimulated emission. Equation (1) is the familiar requirement for population inversion, and is achieved in electron cyclotron masers by constructing an electron gun that produces a beam of electrons whose transverse energy is sharply peaked around some nonzero value.

The condition in Eq. (2) is also realized in electron cyclotron masers since the spacing between quantized energy levels decreases with increasing energy. Solution of the relativistic Schroedinger equation gives the following expression for the electron kinetic energy levels [19]:

$$W_q = mc^2 \left[1+2(q+1/2)\hbar \Omega_o/mc^2\right]^{1/2} - mc^2 \tag{3}$$

where q = 1,2,3...; spin has been neglected; and the nonrelativistic electron cyclotron frequency $\Omega_o = e B_o/m$. It is easily shown that Eq. (3) is equivalent to

$$W_q = (q+1/2)\hbar\Omega_o \; 2/(1+\gamma(q)) \tag{4}$$

where the relativistic energy factor $\gamma(q) = (W_q+mc^2)/mc^2$. The form of Eq. (4) makes clear that relativistic effects serve to decrease the spacing between energy levels as energy increases. In the limit of very large q, where all electron cyclotron masers have operated, the spacing between energy levels becomes $\hbar\omega_{ce}$ where $\omega_{ce} = \Omega_o/\gamma$ is the relativistic electron cyclotron frequency. Incident radiation with frequency slightly larger than ω_{ce} or its harmonics (i.e., $\omega \gtrsim s\omega_{ce}$; s = 1,2,3...) will favor stimulated emission, while $\omega \lesssim s\omega_{ce}$ will favor absorption.

The classical description of the electron cyclotron maser is closely analogous to the quantum mechanical description. In its high power embodiment, the electron cyclotron maser contains an annular beam of electrons that propagates down a drift tube guided by an axial magnetic field, $\underset{\sim}{B}_o$. Each of the electrons has large transverse energy, usually larger than the streaming energy, and so follow a helical path about the magnetic field lines. The Larmor radius, r_L, is usually much smaller than the radius of the annular beam, r_b, so that in cross-section the beam appears as in Fig. 1. In contrast with conventional microwave tubes, the beam diameter may be larger than the wavelength at which amplification occurs (viz., $\lambda \approx 2\pi r_L/\beta_\perp$ where $\beta_\perp$ is the transverse velocity normalized to c). Thus, a large high-power beam is compatible with operation at short wavelengths.

Wave amplification is attributable to phase bunching of the electrons in their cyclotron orbits. In Fig. 1a, the electrons are shown as their interaction with an electromagnetic wave begins. The electrons have almost a single value of transverse energy but are randomly distributed in phase. A wave with an azimuthal electric field will decelerate electron 1 and accelerate electron 2. Thus, initially some electrons lose energy while others gain energy depending on the initial phase of $\underset{\sim}{v} \cdot \underset{\sim}{E}$, and there is no net wave amplification. However, the cyclotron frequency, $\omega_{ce} = eB_o/m\gamma$ is a function of energy. For electron 1 which is decelerated, γ decreases, ω_{ce} increases, and the electron will advance in phase in its cyclotron orbit. Similarly, electron 2 will slip back in phase. The resulting phase bunching will favor wave damping if the wave frequency is slightly smaller than the cyclotron frequency or its harmonics in the reference frame where axial electron energy vanishes ($\omega' \lesssim s\omega'_{ce}$); this is depicted in Fig. 1b.

On the other hand, if $\omega' \gtrsim s\omega'_{ce}$, wave amplification is favored as shown in Fig. 1c. All the electrons are decelerated and lose energy to the wave. Half a cyclotron period later, the net azimuthal motion of the electrons has reversed, but since the phase of the wave also reverses in approximately half a cyclotron period, the wave continues to decelerate the electrons and extract energy. This synchromism between the orbiting electrons and the field implies that in the laboratory frame, the frequency of the wave is approximately equal to the Doppler shifted cyclotron frequency (viz., $\omega \simeq \omega_{ce}+k_z v_z$). Wave amplification is maximized when, in addition, the group velocity equals the axial electron velocity (viz., $\partial\omega/\partial k_z = v_z$).

The electron cyclotron maser can be viewed as a hybrid combining attributes of molecular lasers with attributes of classical microwave tubes, and thereby filling the gap in the electromagnetic spectrum at millimeter and sub-millimeter wavelengths where efficient, high-power coherent sources have been unavailable in the past. Molecular lasers emit at most one photon per molecule; thus, while they are well adapted to generating powerful radiation in the optical and infrared, power generation becomes much more difficult when frequency and photon energy is scaled down toward the millimeter-waveband. On the other hand, classical microwave tubes are based on beams of free electrons, and radiate a huge number of photons per particle with little change in frequency; however, the wavelength of radiation is not a characteristic of the particles but is determined by the physical dimensions of some resonant structure such as a wire helix. Microwave power tubes typically operate at wavelengths of several centimeters. In scaling microwave tubes to smaller wavelengths in the millimeter waveband, the physical dimensions of the tube structure are scaled proportionately smaller and their power handling capacity rapidly diminishes.

The electron cyclotron maser is based on a beam of free electrons and thus emits many quanta per particle. In addition, the frequency is fixed by a characteristic frequency of the particle (i.e., the electron cyclotron frequency) and no small-scale resonant structures are required. Thus, the practical development of the electron cyclotron maser has made possible a leap in power generation capability at millimeter wavelengths.

FIRST OPERATION OF A GYROTRON TRAVELLING WAVE AMPLIFIER

We now proceed to describe the results of initial experiments with a gyrotron travelling wave amplifier. Interactions between radiation in the TE_{01} circular waveguide mode (azimuthal electric field) and the fundamental cyclotron mode of an electron beam were studied. The beam is annular, and is generated by a magnetron injection gun. A careful gun design was performed to create a beam with a velocity distribution which would favor the process [20]. With the ratio of transverse to axial momentum chosen as $p_{\perp o}/p_{zo} = 1.5$, the gun design attempted to minimize momentum spread. A computer analysis of electron trajectories for the chosen gun configuration indicated that momentum spread in the beam would be $2\Delta p_{\perp}/p_{\perp o} \approx \Delta p_z / p_{zo} \approx 10\%$. This beam is propagated down a uniform metallic tube for interaction with an injected r.f. signal. Both gun and tube are placed within a superconducting solenoid, which provides a converging field at the gun, and a uniform field over the interaction region.

The microwave circuit which was used in the experiment is shown in Fig. 2. A driver tube feeds a microwave hybrid which produces two equal signals, 180° out of phase, in rectangular waveguide. These r.f. input signals are injected at two azimuthally opposed positions on the circular drift tube near the gun. Such a configuration launches a TE_{01} wave which propagates in the same direction as the beam (an absorber eliminates the backward moving wave). The interaction between the beam and the radiation can occur over the downstream length of the uniform field, which is 17 cm. Beyond this, the magnetic field rapidly decreases, and the electrons, which are guided by the field lines, are collected on the wall.

The electromagnetic wave continues to propagate down the tube, towards its exit at a vacuum window. Beyond this window, a TE_{0n} mode filter, followed by a mode converter, change the radiation from the TE_{01} circular mode to the fundamental rectangular waveguide mode. Standard waveguide components are then used to evaluate the output radiation.

In order to determine the electronic gain due to the cyclotron maser mechanism, measurements were made of the power coming through the system with the electron beam on, and the beam off. Any effect due to the unoptimized input coupler or wall losses in the drift tube are, thereby, substracted out of the gain measurement.

The optimized design values for this device as taken from reference [18] are listed in Table I. The aim of the designs was to produce an output power of $\geqslant 100$ kW at 35 GHz with good efficiency, gain, and bandwidth. By tuning magnetic field it is possible to trade off efficiency and power for gain and bandwidth. Column (a) gives predicted performance when B_o is chosen to optimize efficiency and column (b) gives predicted performance when B_o is chosen to optimize gain. Both $\Delta p_{\perp}/p_{\perp o}$ and $\Delta p_z/p_{zo}$ were considered to be negligible in these calculations. The geometry and electron beam parameters are held constant for both design (a) and design (b), a 71 kV, 9.5A electron beam being assumed in both cases.

When the device was operated at $I_b > 9$ amps, however, oscillation occurred. Emissions generated in both the TE_{01} forward wave, and the TE_{21} backward wave were identified. This backward wave was measured by detaching the driver tube and measuring the power coupled out through the input waveguide. Amplifier measurements, therefore, were performed at lower currents. The variation of gyro-TWT output as a function of input power level was measured, and is shown in Fig. 3. The lines of constant gain which best fit the data are also plotted. The linear gain shown in Fig. 3 was demonstrated, at 3.5 amps, to extend over a range of at least 30 dB. The systematic wiggles in the experimental data points of Fig. 3 are thought to be due to frequency pulling in the driving source as its output power is varied.

Because the input r.f. does not couple all its power into the growing wave, a careful analysis of the gain process, including the transient effects near the r.f. injection point, is required. We have performed such an analysis and have found that the electric field E(z), at any position z, is given by

$$E(z) = E_0 \left[\sqrt{1+4\cosh(\Gamma z) \cdot (\cosh(\Gamma z)+\cos(\sqrt{3}\Gamma z))} \;/\; 3\right] \quad (5)$$

where E_0 is the initial electric field, and Γ is the spatial growth rate. For $\Gamma L > 1$, we find that the power gain in dB is given by [21]

$$G = -10\log_{10} 9 + 8.686\Gamma L. \quad (6)$$

The first term on the right hand side of Eq. (6) represents the coupling loss due to some of the input radiation exciting waves which do not grow exponentially.

The line through each set of data points in Fig. 3 fixes a measured value of gain from which a growth rate may be determined according to Eq.

(6), using 17 cm as the value for L. The values correspond to growth rates Γ = 0.14, 0.16, and 0.18 cm^{-1} for I_b = 3.5, 6.0, and 7.5 A respectively.

In Fig. 4, output power, P_o, is plotted as a function of B_o, the axial magnetic field in the amplification region, with current held constant at I = 3.5A. The output power peaked at $B_o \simeq$ 13 kG with half power points falling at 12.78 kG and 13.16 kG. This represents an experimental width $\Delta B/B_o$ = 2.9%. The output power was also observed to have a broad peak as V, the electron accelerating voltage, was varied; P_o changed by less than 1 dB as V was swept from 67 kV to 70 kV.

COMPARISON OF EXPERIMENTAL RESULTS WITH THEORY

As discussed in refs. [22] and [23] the wave amplification process is described in cylindrical coordinates (r, θ, z) by a set of three self-consistent equations:

1. the linearized relativistic Vlasov equation,

$$(\partial/\partial t + \underset{\sim}{v} \cdot \partial/\partial \underset{\sim}{x} - e(\underset{\sim}{v} \times \underset{\sim}{B}_o) \cdot \partial/\partial \underset{\sim}{p})f^{(1)}$$
$$= e(\underset{\sim}{E}^{(1)} + \underset{\sim}{v} \times \underset{\sim}{B}^{(1)}) \cdot (\partial/\partial \underset{\sim}{p})f_o \qquad (7)$$

where $\underset{\sim}{v}$ is electron velocity, $\underset{\sim}{p}$ is electron momentum, f_o and $f^{(1)}$ are the equilibrium and perturbed electron distribution functions respectively, and $E^{(1)}$, $B^{(1)}$ are the wave fields of the TE_{on} waveguide mode;

2. the expression for the perturbed beam current density

$$J_\theta^{(1)} = -e\int f^{(1)} v_\theta d^3p; \qquad (8)$$

and

3. the wave equation

$$\omega^2/c^2 - k_z^2 - \alpha_n^2 = \frac{-8\pi\alpha_n \exp(-ik_z z + i\omega t)}{cr_w^2 J_o^2(x_n)} \int rJ_\theta^{(1)} J_1(\alpha_n r)dr \qquad (9)$$

where x_n is the nth non-zero root of $J_1(x) = 0$, r_w is the waveguide radius and $\alpha_n = x_n/r_w$.

To solve these three equations, one must first specify the form of the initial electron distribution function in terms of the constants of motion of the system, namely, the perpendicular and parallel momenta $p_\perp$ and p_z, and the canonical angular momentum P_θ. To be consistent with the experimental configuration that all the electron guiding centers are approximately located on the same cylindrical surface defined by $r = r_o$, we choose f_o to be of the form

$$f_o = K\,\delta\,(r_L^2 - 2P_\theta/eB_o - r_o^2)\;g\,(p_\perp,p_z), \qquad (10)$$

where $\delta(x)$ is the Dirac delta function, $r_L = p_\perp/eB_o$ is the electron Larmor radius, $g(p_\perp,p_z)$ is an arbitrary function of $p_\perp$ and p_z satisfying $\int g d^3p = 1$, and K is a normalization constant chosen to satisfy $\int f_o\, 2\pi r dr d^3p = N$, where N is the number of electrons per unit axial length.

Using the methods of ref. [23], the set of equations (7) through (10) has been solved to yield the following dispersion relation for the interaction between the TE_{on} waveguide mode and the s-th electron cyclotron harmonic.

$$\frac{\omega^2}{c^2} - k_z^2 - \alpha_n^2 = \frac{-8\pi\nu}{\gamma r_w^2 J_o^2(x_n)} \int_o^\infty p_\perp dp_\perp \int_{-\infty}^\infty dp_z g(p_\perp,p_z)$$
$$\cdot\left\{\frac{(\omega^2 - k_z^2c^2)p_\perp^2 H_s(\alpha_n r_o,\alpha_n r_L)}{\gamma^2 m^2 c^2(\omega - k_z v_z - s\omega_{ce})^2} - \frac{(\omega - k_z v_z)Q_s(\alpha_n r_o,\alpha_n r_L)}{\omega - k_z v_z - s\omega_{ce}}\right\} \qquad (11)$$

where $\nu = Nr_e$, $r_e = \mu_o e^2/4\pi m = 2.8\times10^{-12}$ cm is the classical electron radius, $H_x(x,y) \equiv [J_s(x)J_s'(y)]^2$, and $Q_s(x,y) \equiv 2H_x(x,y) + yJ_s'(y)J_s''(y)\{J_s^2(x)(1 + s^2/x^2) + [J_s'(x)]^2\} + 2s^2J_s(x)J_s'(x)J_s'(y)[yJ_s'(y) - J_s(y)]/xy$.

The amplitude growth rate per unit length (Γ) has been solved for numerically from Eq. (11) for the mode and cyclotron harmonic in the experiment (n=s=1) and an assumed Maxwellian momentum distribution,

$$g(p_\perp,p_z) = C \exp\left[-(p_\perp-p_{\perp o})^2/\Delta p_\perp^2 - (p_z-p_{zo})^2/\Delta p_z^2\right],$$

where C is a normalization constant. The values of $Re[\omega]$, r_w, r_o, β_{zo} and $\beta_{\perp o}$ have been chosen to correspond to the experimental values listed in Table I. Voltage and current were chosen as V = 70 kV and I_b = 3.5 A corresponding to the experimental parameters in Fig. 4. In Fig. 5, the calculated values of amplitude growth rate, Γ, are plotted as a function of the axial magnetic field with the beam momentum spread, $T = \Delta p_z/p_{zo} = \Delta p_\perp/p_{\perp o}$, as a parameter.

For ease of comparison with the experimental data of Fig. 3 the growth rate peak has been marked on each curve in Fig. 5. Also marked is the width of each curve, $\Delta B/B_o$, at the points where Γ equals 85% of its peak value; it may be seen from Eq. (6) that a 15% drop in Γ corresponds to a 3 dB decrease in gain when the peak gain is 10.5 dB.

It is observed from Fig. 4 that for a cold beam (T=0) the peak value of Γ (falling at B_o = 13.5 kG) is 0.40 cm^{-1} while $\Delta B/B_o$ = 6.7%. These values are considerable larger than the experimental values (viz., Γ= 0.14 cm^{-1} at $B_o \simeq$ 13.0 kG and $\Delta B/B_o$ = 2.9%). However, the calculated values of peak Γ, the corresponding value of B_o and $\Delta B/B_o$ all decrease as the momentum spread increases. For a momentum spread T =

15%, Fig. 4 shows that the calculated peak value of Γ at B_o = 13.1 kG is 0.16 cm^{-1} while $\Delta B/B_o \simeq 2.7\%$. These calculated values are in good agreement with the experimental data, indicating both the suitability of theoretical model and the fact that electron momentum spread was $T \simeq 15\%$ in the experiment.

Last, we note that the theoretical model outlined above predicts that growth rate will depend on beam current as $\Gamma \sim I_b^{1/3}$ [23]. This dependence of growth rate on current is also borne out by the experimental data of Fig. 3.

DISCUSSION

The linear operation of a gyrotron travelling wave amplifier has been successfully demonstrated over a dynamic range > 30 dB. Although input power was limited and the device was not driven into saturation, the output power level of 10 kW was already high compared with power available from conventional travelling wave amplifiers at 35 GHz.

It was found that experimental parameters could be closely predicted by linear theory. This agreement between experiment and theory was found for the absolute value of gain, the scaling of gain with current and the variation of gain with magnetic field. Thus one has some confidence that other predictions of the linear theory will also be accurate. Specifically, we have now made a preliminary calculation of the bandwidth of the amplifier including a momentum spread of T = 15% in the calculations. We find that for B_o = 13.4 kG the calculated bandwidth is 10% when peak gain is 20 dB; this is only a small degradation from the 11% bandwidth listed in Table I for the case of a cold beam (T = 0). We are in the process of using the non-linear theory to calculate the degradation in efficiency that may be expected with a 15% momentum spread.

A wideband and efficient input coupler is being developed so that the bandwidth and saturated power level may be measured directly. Future work will also include development of multi-stage amplifiers so that higher gain will be demonstrated.

Although at an early stage in its development the gyrotron promises to revolutionize high-power millimeter-wave technology. Gyrotron oscillators are already being effectively applied to controlled thermonuclear fusion research. The first operation of a gyrotron travelling wave amplifier described above indicates that the gyrotron amplifier may prove to be at least as important a device as the oscillator with wide applicability to communications and radar systems.

The authors thank Dr. H. Jory, Mr. R. Lucey and Dr. L. Barnett for helpful discussions and experimental assistance.

REFERENCES

[1] R.Q. Twiss, "Radiation transfer and the possibility of negative absorption in radio astronomy", Aust. J. Phys., vol. 11, pp 564-579, December 1958.

[2] J. Schneider, "Stimulated emission of radiation by relativistic electrons in a magnetic field", Phys. Rev. Letters, vol. 2, pp 504-505, June 15, 1959.

[3] A.V. Gapanov, "Addendum", IZV. VUZ. Radiofizika, vol. 2, no. 5, p. 837, 1959.

[4] G. Bekefi, J.L. Hirshfield and S.C. Brown, "Kirchoff's radiation law for plasmas with non-Maxwellian distributions", Phys. Fluids, vol. 4, pp 173-176, February 1961.

[5] W.E. Lamb, Jr., in Lectures in Theoretical Physics, ed. by C. Dewitt, A. Blandin, and C. Cohen - Tannondji, Gordon and Breach, New York, 1965.

[6] R.H. Pantell, "Backward wave oscillations in an unloaded waveguide", Proc. I.R.E., vol. 47, p. 1146, June 1959.

[7] I.B. Bott, "Tunable source of millimeter and sub-millimeter electromagnetic radiation", Proc. IEEE, vol. 52, pp 330-331, March 1964; also, "A powerful source of millimeter wavelength electromagnetic radiation", Phys. Letters, vol. 14, pp 293-294, February 1965.

[8] J.L. Hirshfield and J.M. Wachtel, "Electron cyclotron maser", Phys. Rev. Letters, vol. 12, pp 533-536, May 11, 1964.

[9] See the following review papers: V.A. Flyagin, A.V. Gapanov, M.I. Petelin and V.K. Yulpatov, "The Gyrotron", IEEE Trans.; Microwave Theory and Technique, vol. MTT-25, pp 514-521, June 1977; and, J.L. Hirshfield and V.L. Granatstein, "The Electron Cyclotron Maser - An Historical Study" ibid. pp 522-527.

[10] N.I. Zaystev, T.B. Pankratova, M.I. Petelin and V.A. Flyagin, "Millimeter and sub-millimeter gyrotrons", Radio Engineering and Electronic Physics, vol. 19, no. 4, pp 95-99, April 1974.

[11] A.A. Andronov, V.A. Flyagin, A.V. Gapanov, A.L. Gol'denberg, M.I. Petelin, V.G. Usov and V.K. Yulpatov, "The gyrotron; high power source of millimetre and submillimetre waves", Infrared Physics, vol. 18, pp 385-394, December 1978.

[12] V.A. Flyagin, private communication.

[13] H. Jory, S. Hegji, J. Shively, R. Symons, "Gyrotron Developments", Microwave Journal, vol. 21, pp. 30-34, August 1978.

[14] M. Read, L. Seftor, R. Lucey, K. R. Chu, J. D. Silverstein and V. L. Granatstein, "A High Power 35 GHz Microwave Source for ECRH", 1978 IEEE International Converence on Plasma Science, Monterey, Calif., 15-17 May, 1978, IEEE Conference Record, 78CH 1357-3 NPS, p. 302.

[15] V. V. Alikaev, G. A. Bobrovskii, V. I. Poznyak, K. A. Razumova, V. V. Sannikov, Yu. A. Sokolov and A. A. Shmarin, "ECR plasma heating in TM-3 Tokamak in magnetic fields up to 25 kOe", Fiz. Plazmy, vol. 2, pp 390-395, 1976 (Sov. J. Plasma Phys., vol. 2, pp 212-215, 1977).

[16] V. L. Granatstein, P. Sprangle, M. Herndon, R. K. Parker and S. P. Schlesinger, "Microwave amplification with an intense relativistic electron beam," J. Appl. Phys., vol. 46, pp 3800-3805, September 1975.

[17] P. Sprangle and A. Drobot, "The linear and self-consistent nonlinear theory of the electron cyclotron maser instability", Trans. IEEE Microwave Theory and Technique, vol. MTT-25, pp 528-544, June 1977; also, P. Sprangle and W. M. Manheimer, "Coherent Nonlinear Theory of a Cyclotron Instability", Phys. Fluids, vol. 18, pp 224-230, February 1975.

[18] K. R. Chu, A. T. Drobot, V. L. Granatstein and J. L. Seftor, "Characteristics and Optimum Operating Parameters of a Gyrotron Travelling Wave Amplifier", IEEE Trans. Microwave Theory and Techniques, vol. MTT-27, pp. 178-187, February 1979.

[19] L. Landau, "Paramagnetism of metals", Z. Phys., vol. 64, p. 629, 1930.

[20] J. L. Seftor, K. R. Chu, A. T. Drobot, "An investigation of a magnetron injection gun suitable for use in cyclotron resonance masers", IEEE Trans. Electron Devices (to be published).

[21] P. Sprangle and R. Smith, "Forward and Backward Wave Operation of the Electron Cyclotron Maser", to be submitted to Physics of Fluids.

[22] M. Friedman, D. A. Hammer, W. M. Manheimer and P. Sprangle, "Enhanced Microwave Emission Due to Transverse Energy of a Relativistic Electron Beam", Phys. Rev. Lett., vol. 31, pp. 752-755, September 1973.

[23] K. R. Chu and A. T. Drobot, "Theory and single wave simulation of the gyrotron travelling wave amplifier operating at cyclotron harmonics", Naval Research Laboratory Memorandum Report 3788, August 1978 (unpublished).

Table I. Parameters from Optimized Designs of Gyrotron Travelling Wave Amplifiers (Cold electron beam)

	(a) Optimized for Maximum Energy	(b) Optimized for Maximum Gain
Magnetic Field, B_o	12.9 kG	13.4 kG
Amplitude Growth Rate, Γ	0.23 cm^{-1} or 2.0 dB/cm	0.53 cm^{-1} or 4.6 dB/cm
Efficiency	51%	22%
Bandwidth (20 dB gain)	2.6%	11%
Output Power, P_o	340 kW	150 kW
Voltage, V	71 kV	
Current, I_b	9.5A	
Frequency, $\omega/2\pi$	35 GHz	
Wall radius, r_w	0.54 cm	
Guiding center radius, r_o	0.25 cm	
Larmor radius, r_L	0.061 cm	
$\beta_{zo} = v_{zo}/c$	0.27	
$\beta_{\perp o} = v_{\perp o}/c$	0.40	

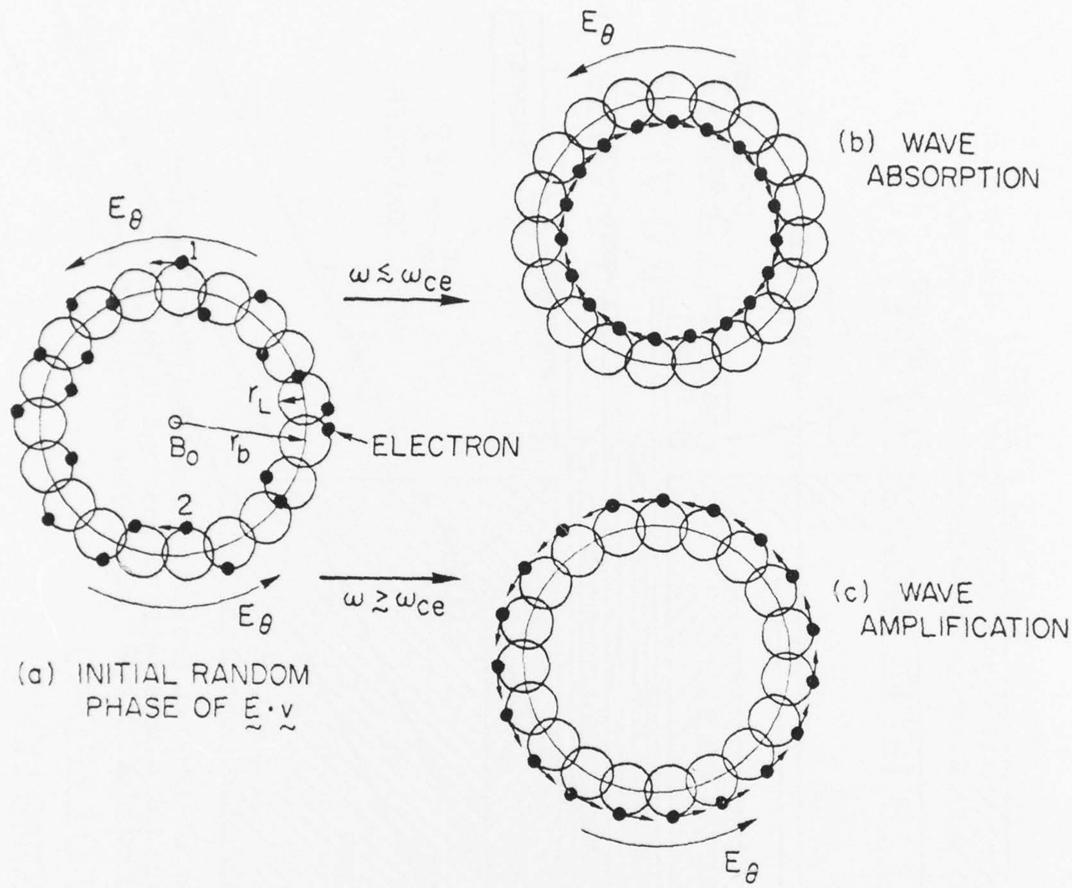

Fig. 1 - A Classical Representation of the Operation of the High Power Electron Cyclotron Maser. Cross-section of annular electron beam is shown. Steady state magnetic field points outward from page.

(a) Initially electrons are oriented randomly in phase with respect to azimuthal electric field of wave E_θ.

(b) When wave frequency is slightly smaller than the electron cyclotron frequency, $\omega \lesssim \omega_{ce}$, electrons become bunched in phase in their cyclotron orbits in such a way as to favor absorption of wave energy.

(c) When $\omega \gtrsim \omega_{ce}$, phase bunching favors wave amplifcation.

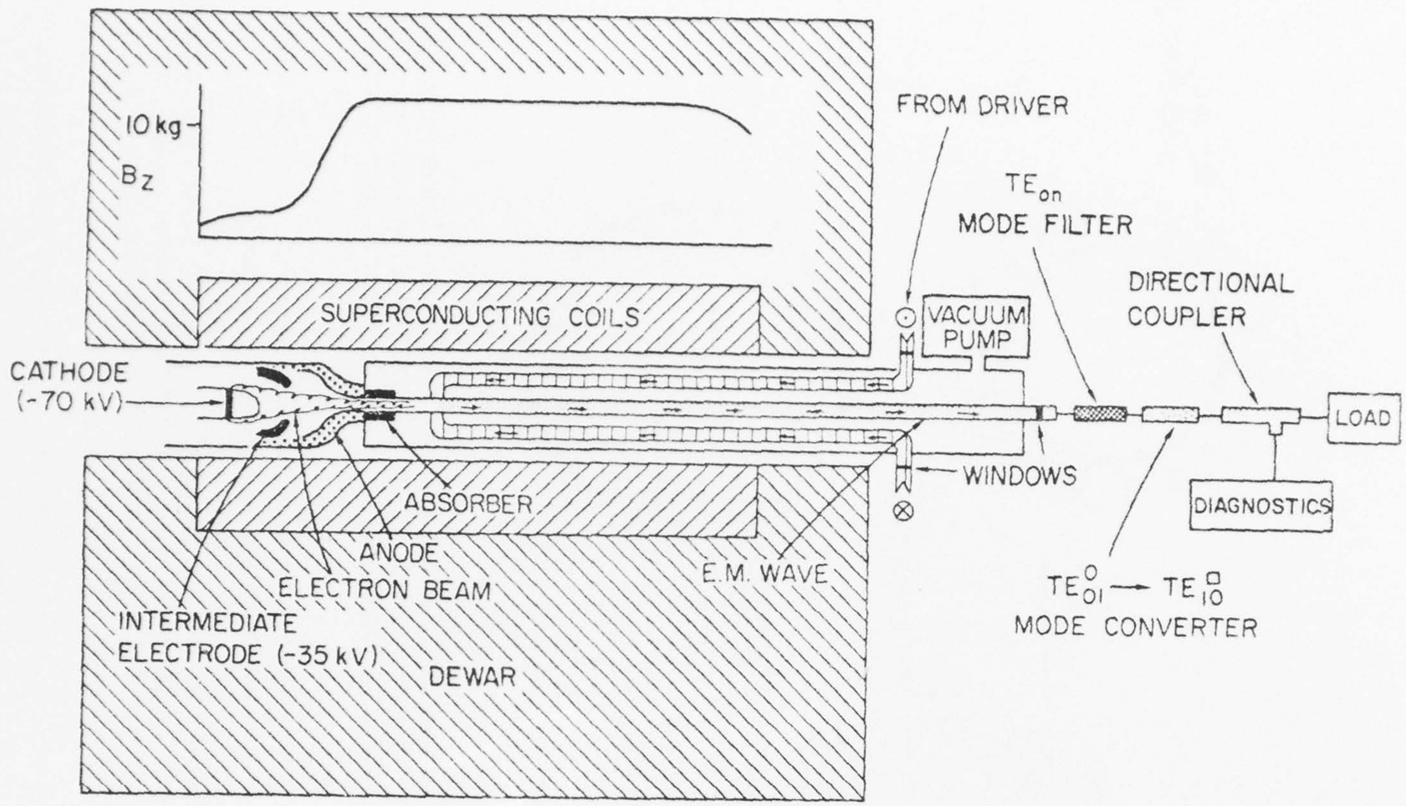

Fig. 2 - Arrangement of Gyrotron Travelling Wave Amplifier Experiment. Electron gun has a thermionic cathode and is pulsed with a repetition rate of 10 sec^{-1} and a pulse width of 1 μsec.

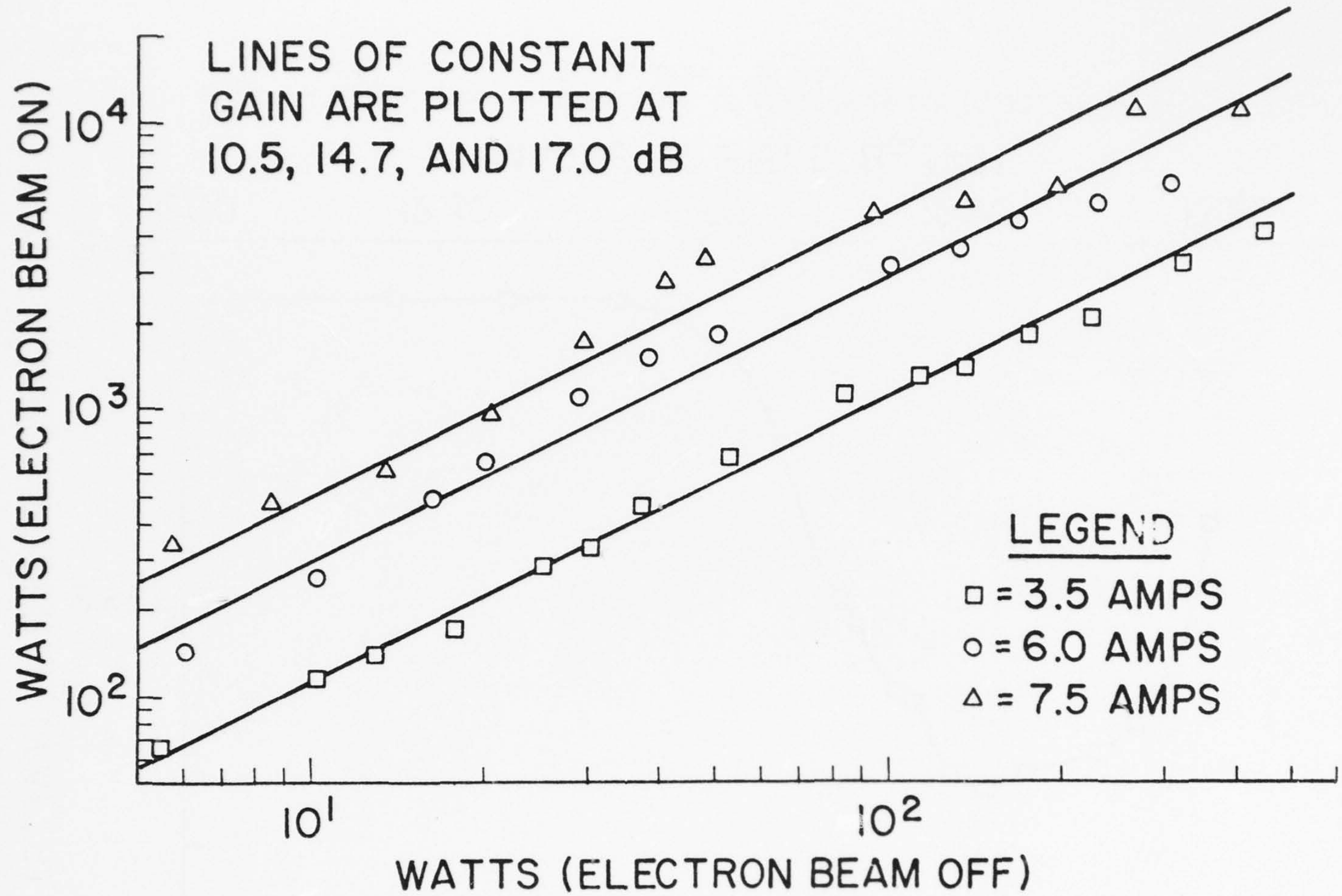

Fig. 3 - Measurement of Gain in the Gyrotron Travelling Wave Amplifier. Output power with electron beam on vs output power with electron beam off ($V = 70$ kV, $B_o = 12.9$ kG, $\omega/2\pi = 35$ GHz).

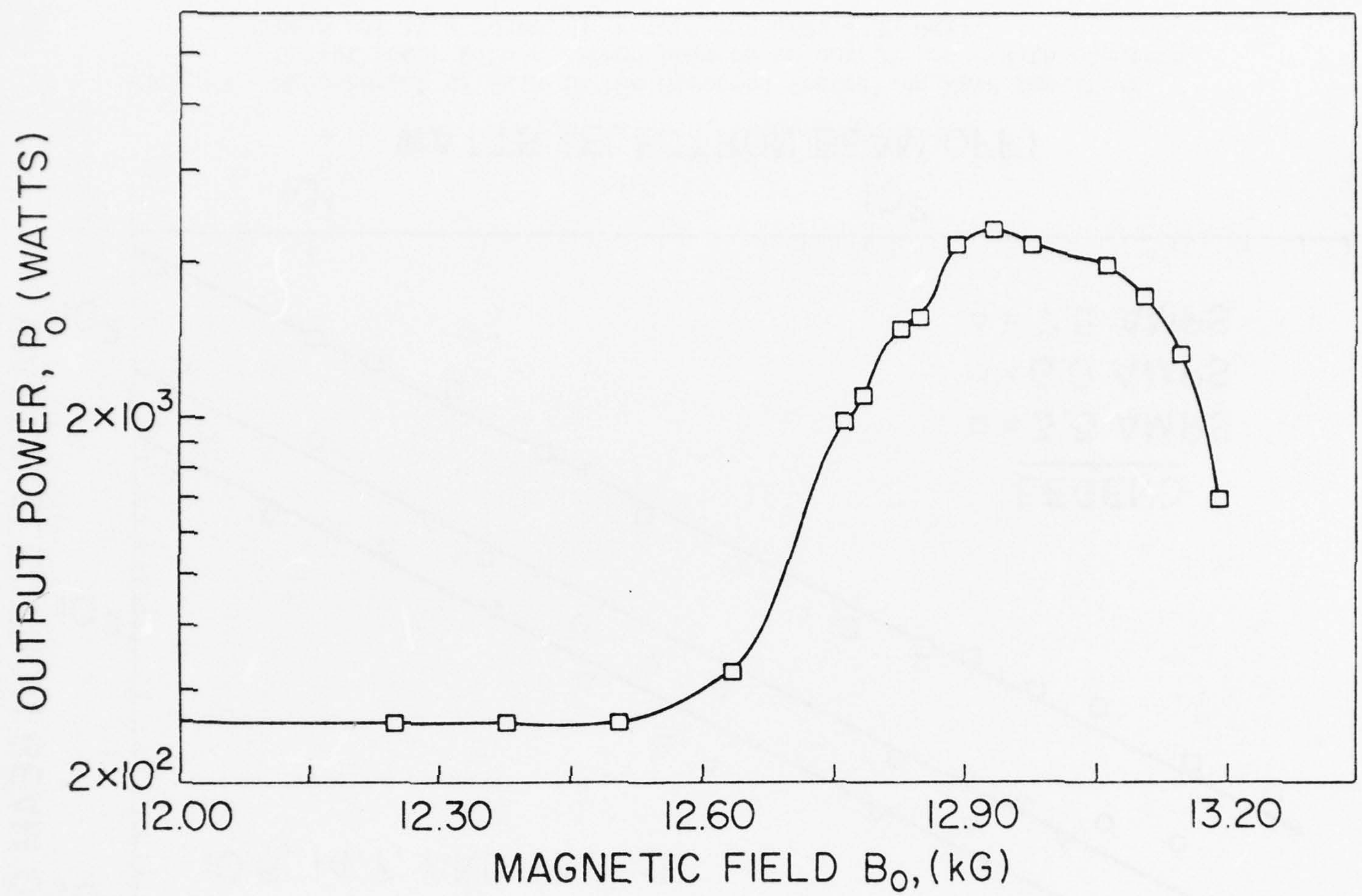

Fig. 4 - Output Power as a Function of Axial Magnetic Field, P_o vs B_o ($V = 70$ kV, $I = 3.5$ A, $\omega/2\pi = 35$ GHz).

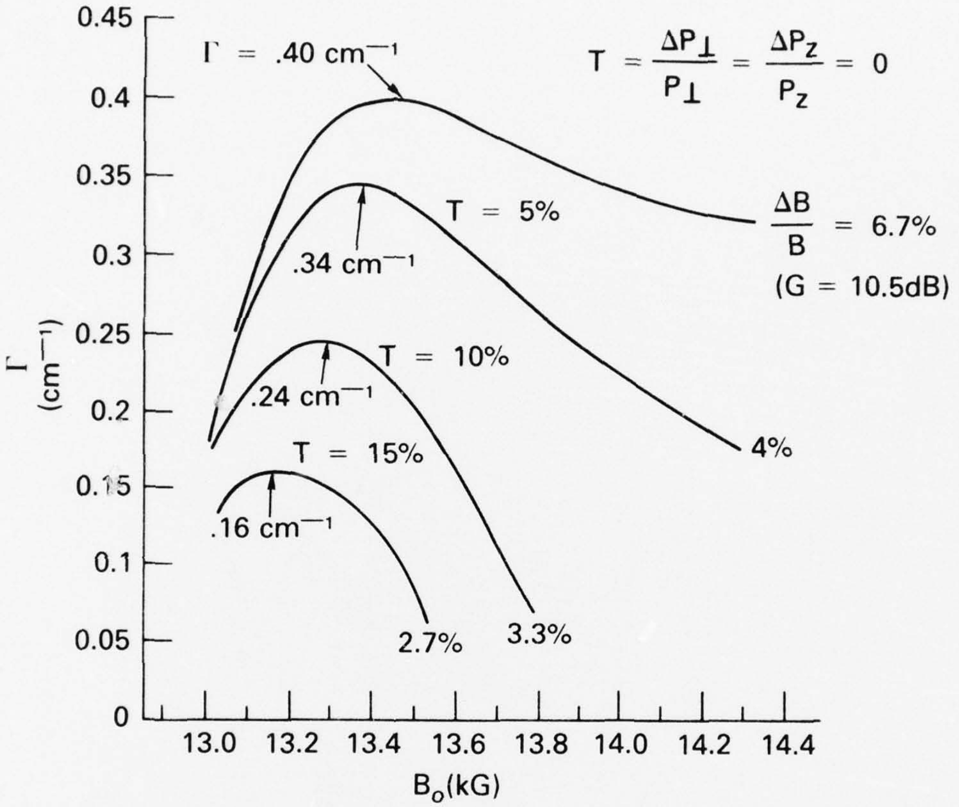

Fig. 5 - Theoretical Calculations of Amplitude Growth Rate, Γ, as a Function of B_o (V = 70 kV, I - 3.5A, $\omega/2\pi$ = 35 GHz).